Accepted Manuscript

Time-resolved velocity of a domain wall in a magnetic microwire

E. Calle, A. Jiménez, M. Vázquez, R.P. del Real

PII: S0925-8388(18)32515-5

DOI: 10.1016/j.jallcom.2018.07.015

Reference: JALCOM 46730

To appear in: *Journal of Alloys and Compounds*

Received Date: 13 March 2018

Revised Date: 29 June 2018

Accepted Date: 2 July 2018

Please cite this article as: E. Calle, A. Jiménez, M. Vázquez, R.P. del Real, Time-resolved velocity of a domain wall in a magnetic microwire, *Journal of Alloys and Compounds* (2018), doi: 10.1016/j.jallcom.2018.07.015.

Time-resolved velocity of a domain wall in a magnetic microwire

E. Calle*, A. Jiménez, M. Vázquez and R.P. del Real

Materials Science Institute of Madrid, CSIC. 28049 Madrid. Spain

ABSTRACT

The dynamic process of nucleation, propagation, and braking of a single domain wall (DW) has been systematically determined in a Fe-based magnetostrictive microwire under an applied axial magnetic field. While in previous reports the Sixtus-Tonks experiments have provided partial information on the process (i.e., the average velocity), in the present study we report on the instantaneous processes involved in the propagation of the DW, as well as the transient process during the DW depinning. The experimental measurements were carried out using the spontaneous Matteucci effect induced during DW propagation due to the small helical magnetization component created during the fabrication process.

Keywords: Magnetic microwire, Time-resolved domain wall velocity, Amorphous materials, Electromotive force, Magnetisation, Magnetostriction

1. Introduction

Amorphous glass coated microwires (AGCMs) [1] show excellent magnetic softness and very good mechanical properties which make them very suitable for many technological applications such as magnetic, temperature or stress sensors [2, 3] or for the fabrication of metamaterials [4]. Magnetoelastic anisotropy is the most important parameter that determines their magnetic properties. Its origin is the coupling between the magnetostriction constant and the stresses induced during the fabrication process due to the difference in the thermal expansion coefficients of the glass and the magnetic material. Fe-based AGCMs show a large magnetoelastic anisotropy due to their magnetostriction constant ($\lambda \sim 10^{-5}$). This anisotropy confers them a bistable magnetic behaviour characterized by a square hysteresis loop with a Barkhausen jump: the magnetization of the wire takes place by the depinning and propagation of a domain wall (DW) [5] from one end of the microwire when an axial magnetic field is applied. Coercive field, remanent magnetization, and high frequency behaviour can be improved by controlling the conditions (temperature and time) of a stress annealing of the microwire [6-8].

This bistability makes it possible to study the propagation of a single DW. Its motion has been widely studied including its average velocity as a function of the magnetic field and stress applied [9], the acceleration and braking of the DW by local magnetic fields (parallel and antiparallel to the main applied field) [10], and the nucleation of a reverse domain and propagation of the two DW's head-to-head and tail-to-tail in opposite directions [11]. All these measurements have been traditionally based on a classical Sixtus-Tonks system with several pickup coils that permits us to identify the direction of the DWs motion and determine the DW

*Corresponding author.
e-mail address: esther.calle@csic.es

velocity from the time interval between the peaks induced in the pickup coils, provided the distance between them is known.

The Matteucci and inverse Wiedemann effects are two well-known phenomena exhibited by Fe-based AGCMs and in general by magnetostrictive materials. Both effects are related to crossed hysteresis loops (i.e., non-diagonal terms of the susceptibility tensor), in which the magnetization is measured along a direction transverse to that of the applied magnetic field: for the cylindrical geometry of microwires M_ϕ vs. H_z and M_z vs. H_ϕ hysteresis loops [12,13]. The Matteucci effect consists of the appearance of a voltage induced at the ends of a wire under an ac axial field which is a consequence of a helical magnetic anisotropy in a material subjected to a torsional stress resulting in a change of the azimuthal component of magnetization when an axial field is applied. The Wiedemann effect consists of the observation of a magnetostrictive torsion when a helicoidal magnetic field is applied, which can be achieved by passing a current through the material while simultaneously applying an axial magnetic field.

As a consequence of the spontaneous helical anisotropy introduced during the microwire's fabrication process, it is possible to measure the Matteucci effect during the propagation of a single DW under an applied axial magnetic field, without needing to apply a torsional stress. This fact has permitted us to obtain time-resolved information on the DW velocity during its propagation, providing a deeper understanding of the DW motion in comparison with the classical Sixtus-Tonks system used for studying the DW dynamics in these materials so far. Similar time-resolved information of the DW motion up until now has only been achieved in nanowires and nanostripes, by means of different methods, as anisotropic magnetoresistance [14], time-resolved XMCD microscopy [15] and waveguide-type antenna measurements [16].

2. Experimental setup

The glass coated microwire was prepared in our laboratory by using the Taylor-Ulitovsky method [17] with a composition of $Fe_{75}Si_{10}B_{15}$, 19 microns in diameter of the metallic nucleus, around 1 micron of glass cover (total diameter of 20,5 microns), and a length of 41,9 cm. An optical image of the microwire morphology is shown in Fig. 1(a). The structure of the studied microwire was checked using a Bruker (D8 Advance A25) X-ray diffractometer with Cu K_α radiation (wavelength=1,54Å). The X ray diffraction pattern [Fig. 1(b)] shows a broad hump around 45º which demonstrates that the wire is amorphous. Furthermore, the hysteresis loop (coercive field H_c=50 A/m) measured with a vibrating sample magnetometer [Fig. 1(c)] shows a large Barkhausen jump related with the propagation of a single DW.
The magnetostriction of the sample is $35 \cdot 10^{-6}$ ppm[18]. This large value, along with the stresses induced by the glass coating, are the origin of the magnetoelastic anisotropy; for the same metallic diameter, a thicker coating yields a larger anisotropy and a smaller DW velocity [19,20].

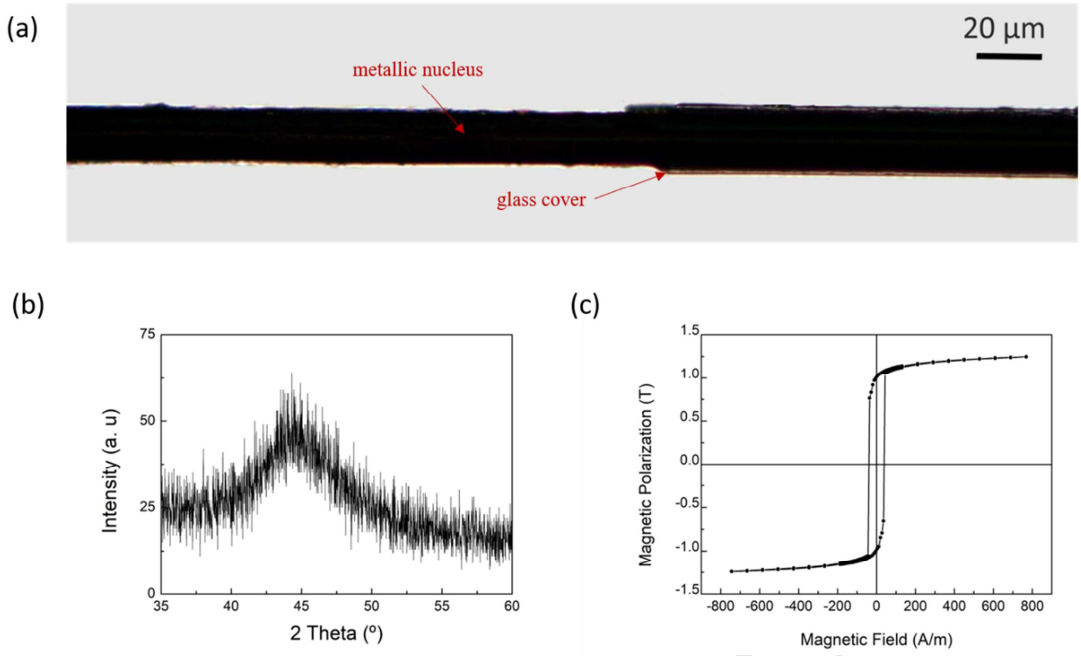

Fig. 1. (a) Optical image showing the morphology of the studied microwire: on the left side the glass cover has been removed showing only the metallic nucleus. (b) XRD pattern. (c) Hysteresis loop of the amorphous microwire.

The setup to measure the DW velocity uses a coil to apply an axial magnetic field with a field constant of 2227,9 m^{-1}. One end of the microwire was placed inside the coil and the other one outside in order to ensure the propagation of a single DW depinned from the end inside the coil [see Fig. 2(a)]. A Tektronix AFG3252 arbitrary function generator was used to apply a 31 hertz square waveform to the coil to produce the depinning and propagation of the DW. A non-inductive resistor was placed in series to measure the applied magnetic field. In order to measure the electromotive force induced in the microwire during the DW propagation, electrical contacts were made with silver paint at the ends of the microwire after mechanical removal of the glass coating. The e.m.f. was amplified with a Standford Research System Model SR560 amplifier using a gain factor of 500.

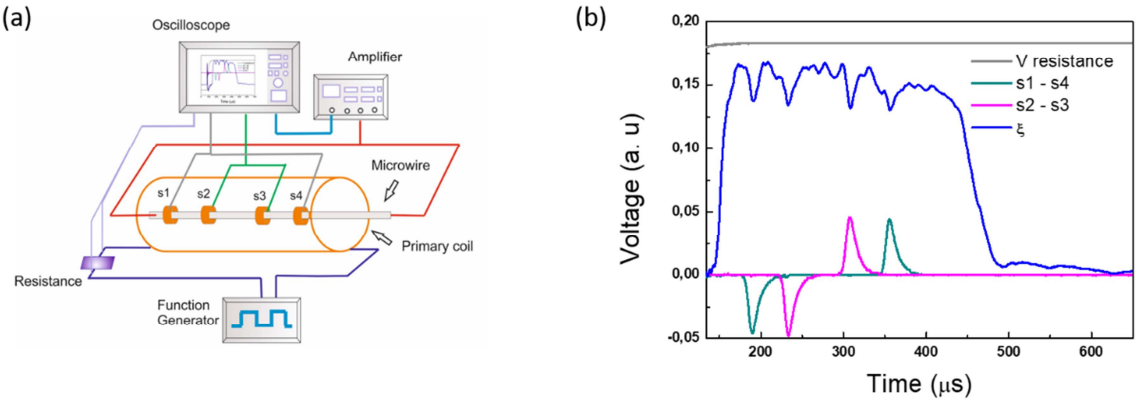

Fig. 2. (a) Schematic view of the experimental setup used for the simultaneous Matteucci effect and Sixtus-Tonks measurements. (b) Voltage signals measured in the four channel oscilloscope.

In order to correlate the e.m.f. induced and the velocity of the DW, the experimental setup contains a Sixtus-Tonks system with four pickup coils. The pickup coils each had 2000 turns and a length of 3mm. The distance separating the pairs s1-s2 and s3-s4 was 5 cm, and the

distance separating the pair s2-s3 was 8,4 cm [see Fig. 2(a)]. The time sequence of the signals of the pickup coils demonstrates the existence of only one DW during the experiment.

The voltage in the resistor, the e.m.f. signals from the pickup coils (opposite-series connected) and the e.m.f. induced at the ends of the wire were measured with a Tektronix TDS3034B four channel oscilloscope, ensuring that the depinning and propagation of the DW occurred when the applied magnetic field had reached a constant value.

3. Results and discussion

The helical anisotropy resulting from the introduced stress during the fabrication process is responsible for the existence of an azimuthal component in the magnetization of the wire that varies during magnetization reversal due to the propagation of the DW. According to Faraday's law of electromagnetic induction this results in the appearence of an e.m.f., ξ, at the ends of the microwire that can be expressed as:

$$\xi = 2\mu_0 M_\varphi r v_{DW}(t) \qquad (1)$$

where M_φ is the azimuthal component of magnetization, r the radius of the metallic nucleus of the microwire, and v_{DW} the DW velocity. This means that ξ as a function of time during DW propagation will give us novel, time-resolved information about the propagation of the DW for samples showing small variations in either r or M_φ. Up to now all the reported studies concerning DW dynamics in AGCM have been performed with a Sixtus-Tonks system, which provides information about the average DW velocity between pairs of points in the microwire where the pickup coils are placed. Whatever happens between the points where the pickup coils are located is uncertain, as well as the processes of generation, acceleration, and braking of the DW.

Fig. 2(b) shows ξ and the voltages from the four Sixtus-Tonks coils. A first abrupt peak (not shown) is observed in ξ due to the sharp change in magnetic flux during the inversion of the applied magnetic field. For the measurements we chose a microwire for which at that time the DW formation has not started yet, so this peak does not mask ξ due to the DW.

The ratio between the value of ξ and the DW velocity, 1873,4 m/(Vs), has been determined from the relationship between the average DW velocity (obtained from the time interval between the induced peaks in the pickup coils s1 and s4) and the average of ξ measured in the same time interval. From here, using this constant and eq. (1) we have obtained the average value of the azimuthal magnetization due to the fabrication process, $\mu_0 M_\varphi = 5{,}59 \cdot 10^{-2}$ T. As $\mu_0 M_s = 1{,}43$ T, the twisting angle is around 2,2 degrees.

The time-resolved DW velocity is shown in detail in Fig. 3(a) for an applied field of 67,9 A/m. Three different regions can be observed: in region (I) a sudden increase is measured due to acceleration of the DW after its creation. In region (II) the DW reaches a steady regime with some variations that will be discussed next, and finally, in region (III) the DW leaves the primary coil and experiences a braking until it is completely stopped due to the decreasing of the magnetic field.

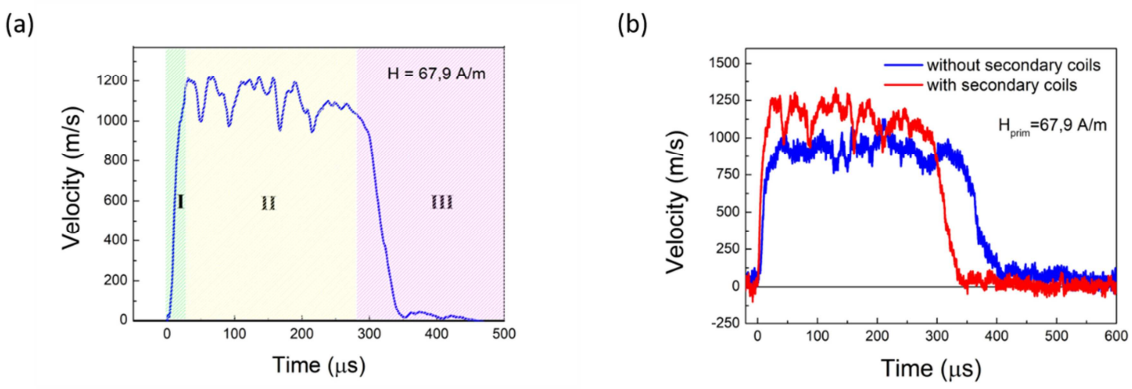

Fig. 3. (a) Three regions in the time-resolved DW velocity that can be associated to the acceleration (I), propagation (II) and final braking of the DW when it leaves the primary coil. (b) Comparison of measurements of the instantaneous DW velocity with/without pickup coils for the same applied magnetic field H= 67,9 A/m.

In region II in Fig. 3(a) some pronounced valleys can be observed coinciding with the peaks induced in the pickup coils, as it was shown in Fig. 2(b), representing a reduction in the velocity by around 20% and indicating the braking of the DW when passing through these pickup coils due to the generated counter-magnetic field. This means that in previous studies on DW dynamics the DW velocity was being underestimated as a consequence of the braking produced by the very setup used to measure. In particular, for the microwire studied here the underestimation is around 6%.

Trying to avoid the braking of the DW, new measurements were made without those coils, by placing the microwire in the same position with respect to the primary coil as in the former measurements [Fig. 3(b)]. Different amplitudes and durations of ξ were obtained for the same applied magnetic field comparing the system with and without pickup coils. It could be related to the different stress and torsion applied on the microwire during the fixing of its position, which could modify the value of the helical anisotropy.

For the calculation of the DW velocity in the system without pickup coils, we have considered that the distance travelled by the DW was the same as that found in the measurement with pickup coils, i.e. 33,88 cm. Dividing this distance by the integral of ξ in the range of time in which DW is moving, we obtained that the ratio between the DW velocity and ξ was 2213.36 m/(Vs). In this case, $\mu_0 M_\varphi = 4{,}6 \cdot 10^{-2}$ T and the twisting angle is 1,8 degrees. This means that due to the high value of microwire magnetostriction, an axial stress is applied and therefore the total twisting angle is smaller.

In order to study the DW kinetics we have considered the DW as a punctual mass which motion can be described by the following equation:

$$m\frac{d^2x}{dt} + \beta\frac{dx}{dt} + kx = 2\mu_0 M_S S H \qquad (2)$$

where x represents the DW position, m the DW mass, β the damping coefficient, k the restoring coefficient, S the wire section, and H the applied magnetic field.

Considering that the restoring force has a homogeneous effect that acts onto the DW as an effective threshold field, which is necessary to overcome for propagation, equation (2) can be expressed as:

$$m\frac{dv}{dt} + \beta v = 2\mu_0 M_S S\left(H - H_{fr}\right) \qquad (3)$$

where v is the velocity of the DW and H_{fr} represents the threshold or friction field for the depinning and propagation of a DW that is already generated.

When the DW reaches a constant velocity, it can be expressed as follows [21]:

$$v = (2\mu_0 M_S S/\beta)(H - H_{fr}) \qquad (4)$$

The magnetic field generated by the primary coil has the following theoretical dependence on the x-coordinate:

$$H = \frac{NI}{2l}\left[\frac{x + l/2}{\sqrt{(x + l/2)^2 + a^2}} - \frac{x - l/2}{\sqrt{(x - l/2)^2 + a^2}}\right] \qquad (5)$$

where I is the current through the primary coil, l the length, N the number of turns, and a the radius. The origin of x-coordinate is placed at the center of the primary coil.

In order to determine the minimum field necessary to propagate a DW that is already generated along the wire (H_{fr}), a variable magnetic field (Fig. 4) was applied to the primary coil. That magnetic field consisted of a first pulse higher than the switching field (region A), followed by a zero field (region B), and then by a region in which a constant magnetic field lower than the switching field was applied (region C). That permitted us to create and move the DW at a certain position along the wire, then stop it when the magnetic field went to zero, and finally move it again at a lower field. Varying the value of the magnetic field applied in region C it is possible to determine the minimum (20,49 A/m) and maximum (24,06 A/m) value of H_{fr} (to start moving the DW and to move it through the whole wire respectively).

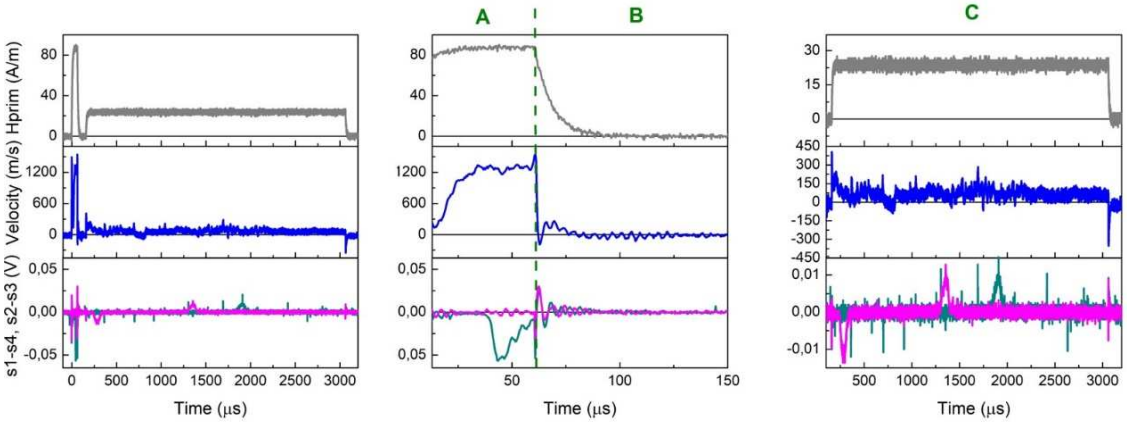

Fig. 4. From up to down: applied magnetic field, instantaneous velocity, and induced voltages in the pairs of pickup coils s1-s4 and s2-s3. The graph on the left side represents a complete semi-period showing the time dependence of the applied magnetic field and the induced e.m.f. signals. In the graph at the center two regions can be distinguished: region A in which the DW is first generated at a high magnetic field and moves for a while, and region B in which the DW stops due to the decrease in magnetic field. The graph on the right side represents region C in which the already generated DW starts from rest and propagates through the whole wire (applied field 24 A/m).

In order to obtain the value of β from equation (4), we calculate the average values of H_{fr} and v in region II [Fig. 3(a)], for an applied field H_{app}=67,9 A/m, resulting in β= 3,66·10^{-11} Ns/m.

After introducing all these parameters into the differential equation (3), it was solved by means of MATLAB R2010b, using the code45 algorithm for the Runge-Kutta method. The DW mass, m=1,819·10^{-16} kg, was obtained after matching the theoretical and experimental instantaneous velocities.

Both experimental and theoretical curves of instantaneous velocity for the measurement performed at 67,9 A/m without pickup coils can be seen in Fig. 5(a). The theoretical fit reproduces the experimental curve quite well. It can be observed in the inset in Fig. 5(a) that the region (I) can be divided in two sub-regions of different slopes: a) region (I.a) lasts around 8 μs, with a smaller slope which is probably related to the formation of the DW or to a time with a different propagation that does not fit with our model (this would mean that the DW takes some time to behave like a punctual mass); and b) region (I.b) that it is related to the acceleration of the DW until it reaches the steady velocity, taking around 20 μs. The formation and acceleration times show the dramatic influence of the DW mass on the dynamics. As a comparison, it is worth keeping in mind that the mass of a DW in a nanostripe is around seven orders of magnitude smaller [22] and the time needed to reach the steady velocity is only few nanoseconds [23].

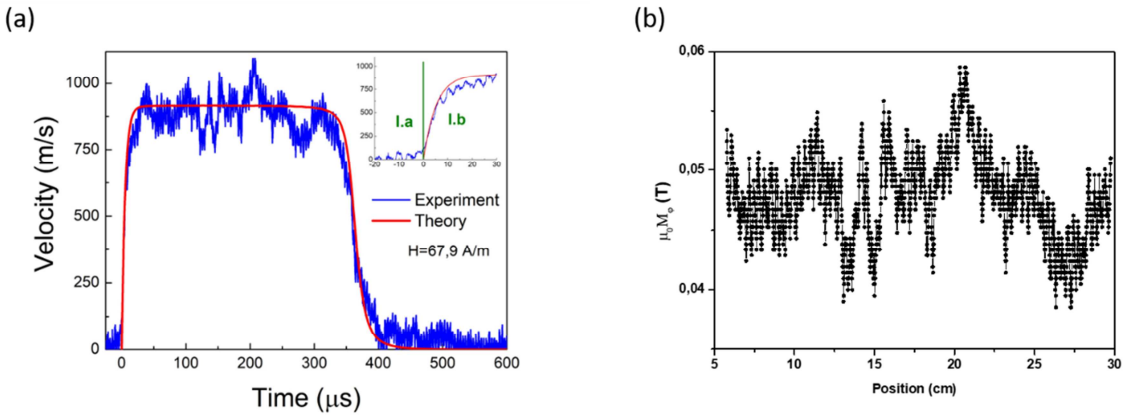

Fig. 5. (a) Experimental and theoretical curves of instantaneous velocity for the measurement performed without pickup coils. Inset shows those curves until the DW reaches the steady velocity. (b) Spatial variation of the azimuthal magnetic polarization in region II assuming a constant velocity of the DW.

As the position with respect to the primary coil and the length of the microwire in the experiment were well known, it was possible to estimate the initial position of the center of mass of the DW, which was found to be 2,85 cm from the end of the microwire from which the DW depins.

The fitting curve between 40 and 300 μs (region II) shows a constant velocity. However, the experimental values present spatial variations. In contrast to regions I and III (where ξ varies mainly due to DW velocity), the variations in ξ (eq. 1) in region II can be due to r, M_ϕ, or the DW velocity. In order to check the influence of the diameter, the metallic core of the microwire was measured along the wire with an optical microscope. Some punctual inhomogeneities were found which do not match the variations in ξ, permitting us to discard the inhomogeneity in diameter as the main cause of the fluctuations in ξ.

The variations in the DW velocity are related to β through eq (4). The damping experienced by the DW during propagation is the sum of a few different contributions [24]. One is due to eddy currents and depends on geometrical factors, therefore, variations in the eddy current damping could be related to a non-homogeneous diameter of the microwire as well as with variations in resistivity [25]. However, it would give us the theoretical DW velocities one order of magnitude larger than the experimental ones [26], meaning that eddy-current contribution can be neglected in microwires due to its high resistivity and small diameter. Another contribution to β is

associated with mobile defects existing in the amorphous matrix that can interact, hindering the DW during its propagation if its relaxation frequency is in the range of frequency of the applied magnetic field. Several studies have been done about the dependence of the damping mechanism on temperature, frequency, and tensile stress [24,27,28]. In our measurements the frequency of the applied magnetic field was 31 Hz, which is a low frequency, so could be expected that the defects had enough time to relax and therefore to contribute to the damping of the DW via the structural relaxation. Some spatial variations in the damping coefficient related to structural relaxation could then occur as a consequence of a different concentration of mobile defects along the length of the wire. We have not, however, measured differences in ξ as a function of the frequency of the applied magnetic field in the 1Hz-6 kHz range, which means the DW damping cannot be due to structural relaxation.

Another term in the damping coefficient is related to the magnetic relaxation due to the rotation of the spins which form the DW. In this case $\beta \propto (K)^{1/2}$ where K is the magnetic anisotropy of the microwire. Due to the fabrication process, small local variations of the glass coating's thickness could produce variations in the stress applied and therefore in the magnetoelastic anisotropy. From eq.(1) it is difficult to obtain detailed information because K somehow affects both M_ϕ and v (through β and the pinning field H_{fr}). As a first approach we can assume that the DW velocity is constant in region II. Fig. 5 (b) shows the variation of the azimuthal magnetic polarization of the microwire in this region under this assumption. From these values we obtain that the twisting angle goes from 1,5 to 2,3 degrees.

On the other hand, some studies on the distribution and role of defects in amorphous bistable microwires have been performed in which the authors have studied the distribution of the local nucleation fields, obtaining a shape similar to that of Fig. 5 (b) [29]. The advantage of the Matteucci effect is that it is possible to instantaneously obtain the information of the whole wire.

4. Conclusions

The present measurement of the Matteucci effect has been able to unveil the different stages of the DW from its depinning until its braking, as well as local deviations from its average velocity when it is moving between the pickup coils. Performing a theoretical study of the measured instantaneous velocity made it possible to estimate the time needed for DW generation as well as the initial position of its center of mass.

The instantaneous measurement of the DW velocity has allowed us to realise the interaction between the propagating DW and the pickup coils. By measuring the Matteucci effect in a system without pickup coils we have avoided the undesirable local braking created by them, but the measured velocity still varies in the region in which it should be constant. We think these deviations from the average velocity could be due to the spatial dependence of the magnetoelastic anisotropy.

From the point of view of technological applications, the study of the instantaneous DW motion is very important in order to understand and improve the operating features of many devices based on DW logic.

Acknowledgements

This work was supported by the Spanish National Research Council under CSIC Project No. 201760E040. E. Calle acknowledges T. Sánchez for her help with the XRD measurements, and C. Bran and A. C. Jimenez for their careful reading of the manuscript.

Declarations of interest: none

Author contributions

E. Calle, R. P. del Real and M. Vázquez conceived the idea of the manuscript. E. Calle and A. Jiménez prepared and chararacterized the studied glass coated microwire and performed the simultaneous Sixtus-Tonks and Matteucci effect measurements. The theoretical DW velocity was calculated by E. Calle and R. P del Real. The main text was written by E. Calle, R. P. del Real and M. Vázquez. All authors reviewed and approved the final version of the manuscript.

References

[1] S. A. Baranov, V. S. Larin, A. V. Torcunov, Technology, Preparation and Properties of the Cast Glass-Coated Magnetic Microwires, Crystals 7(6) (2017) 136

[2] R. Varga, P. Klein, R. Sabol, K. Richter, R. Hudak, I. Polacek, D. Praslicka, M. Smelko, J. Hudak, I. Mikita, G. A. Badini-Confalonieri, R. E. Kammouni, M. Vazquez, Magnetically Bistable Microwires: Properties and Applications for Magnetic Field, Temperature, and Stress Sensing, in: A. Zhukov (Ed.), High performance soft magnetic materials, Springer Series in Materials Science 252, 2017, pp. 169-212

[3] M. Churyukanova, S. Kaloshkin, E. Shuvaeva, A. Stepashkin, M. Zhdanova, A. Aronin, O. Aksenov, P. Arakelov, V. Zhukova, A. Zhukov, Non-contact method for stress monitoring based on stress dependence of magnetic properties of Fe-based microwires, J. Alloys Compd. 748 (2018) 199-205

[4] V. Lopez-Dominguez, M. A. Garcia, P. Marin, A. Hernando, Tuning Metamaterials by using Amorphous Magnetic Microwires, Sci. Rep. 7 (2017) 9394

[5] F. Beck, J.N. Rigue, M. Carara, The profile of the domain walls in amorphous glass-covered microwires, J. Magn. Magn. Mat. 435 (2017) 21-25

[6] V. Zhukova, J. M. Blanco, M. Ipatov, M. Churyukanova, S. Taskaev and A. Zhukov, Tailoring of magnetoimpedance effect and magnetic softness of Fe-rich glass-coated microwires by stress-annealing, Sci. Rep. 8 (2018) 3202

[7] V. Zhukova, M. Ipatov, A. Talaat, J.M. Blanco, M. Churyukanova, A. Zhukov, Effect of stress annealing on magnetic properties and GMI effect of Co- and Fe- rich microwires, J. Alloys Compd. 707 (2017) 189-194

[8] A. Zhukov, M. Ipatov, M. Churyukanova, A. Talaat, J.M. Blanco, V. Zhukova, Trends in optimization of giant magnetoimpedance effect in amorphous and nanocrystalline materials, J. Alloys Compd. 727 (2017) 887-901

[9] V. Zhukova, J.M Blanco, V. Rodionova, M. Ipatov, A. Zhukov, Fast magnetization switching in Fe-rich amorphous microwires: Effect of magnetoelastic anisotropy and role of defects, J. Alloys Compd. 586 (2014) S287-S290

[10] M. Vázquez, G. A. Basheed, G. Infante and R.P. del Real, Trapping and injecting single domain walls in magnetic wire by local fields, Phys. Rev. Lett. 108 (2012) 037201

[11] A. Jiménez and M. Vázquez, Alternating motion of Single-Domain Walls in Uniaxial Magnetic Wire, IEEE Magn. Lett. 5 (2014) 5000204

[12] M. Ipatov, V. Zhukova, A. Zhukov, J. González, Magnetoimpedance sensitive to dc bias current in amorphous microwire, Appl. Phys. Lett. 97 (2010) 252507

[13] M. Ipatov, V. Zhukova, J. González, A. Zhukov, Manipulating the magnetoimpedance by dc bias current in amorphous microwire, J. Magn. Magn. Mat. 324 (2012) 4078-4083

[14] M. Hayashi, L. Thomas, Ya. B. Bazaliy, C. Rettner, R. Moriya, X. Jiang, S. S. P. Parkin, Influence of current on field-driven domain wall motion in permalloy nanowires from time resolved measurements of anisotropic magnetoresistance, Phys. Rev. Lett. 96 (2006) 197207

[15] F.-U.Stein, L. Bocklage, M. Weigand, G. Meier, Time-resolved imaging of nonlinear magnetic domain-wall dynamics in ferromagnetic nanowires, Sci. Rep. 3 (2013) 1737

[16] M. Hayashi, S. Kasai, S. Mitani, Time resolved inductive detection of domain wall dynamics in magnetic nanowires, Appl. Phys. Express 3 (2010) 113004

[17] H. Chiriac, Preparation and characterization of glass covered magnetic microwires, Mater. Sci. Eng. A 304-306 (2001) 166-171

[18] H. Fujimori, K. I. Arai, H. Shirae, H. Saito, T. Masumoto, N. Tsuya, Magnetostriction of Fe-Co amorphous alloys, Japan J. Appl. Phys. 15(4) (1976) 705-706

[19] V. Zhukova, J.M. Blanco, M. Ipatov, A. Zhukov, Domain wall dynamics of magnetically bistable microwires, EPJ Web Conf. 29 (2012) 00036

[20] S. Corodeanu, T. Óvári, H. Chiriac, Effect of In Situ Glass Removal on the Magnetic Switching in Amorphous Microwires, IEEE Trans. Magn. 50 (11) (2014) 2007204

[21] B.D. Cullity and C.D. Graham, Introduction to magnetic materials, 2nd ed., Wiley and IEEE Press, 2009

[22] E. Saitoh, H. Miyajima, T. Yamaoka, G. Tatara, Current-induced resonance and mass determination of a single magnetic domain wall, Nature 432 (2004) 203-206

[23] M. Hayashi, L. Thomas, C. Rettner, R. Moriya, S. S. P. Parkin, Direct observation of the coherent precession of magnetic domain walls propagating along permalloy nanowires, Nat. Phys. 3 (2007) 21-25

[24] K. Richter, R. Varga, A. Zhukov, Influence of the magnetoelastic anisotropy on the domain wall dynamics in bistable amorphous wires, J. Phys. Condens. Matter 24 (2012) 296003

[25] D.-X Chen, N. M. Dempsey, M. Vázquez, A. Hernando, Propagating domain wall shape and dynamics in iron-rich amorphous wires, IEEE Trans. Magn. 31 (1) (1995) 781-790

[26] R.P. del Real, C. Prados, D.-X. Chen, A. Hernando, M. Vázquez, Eddy current damping of planar domain wall in bistable amorphous wires, App. Phys. Lett. 63 (25) (1993) 3518-3520

[27] G. Infante, R. Varga, G. A. Badini-Confalonieri, M. Vázquez, Locally induced domain wall damping in a thin magnetic wire, Appl. Phys. Lett. 95 (2009) 012503

[28] R. Varga, G. Infante, G. A. Badini-Confalonieri, M. Vázquez, Diffusion-damped domain wall dynamics, J. Phys: Conf. Ser. 200 (2010) 042026

[29] A. Zhukov, J. M. Blanco, M. Ipatov, V. Rodionova, V. Zhukova, Magnetoelastic effects and distribution of defects in micrometric amorphous wires, IEEE Trans. Magn. 48 (4) (2012) 1324-1326

- The velocity of a single domain wall is time-resolved in microwires.
- The domain wall dynamics is instantaneous and locally determined along the wire.
- The processes of nucleation, depinning and braking of the wall are identified.
- Matteucci effect is employed to measure the domain wall velocity.